



ThDIGI17

## Super Resolution of Fault Plane Prediction by a Generative Adversarial Network

F. Jiang<sup>1\*</sup>, P. Norlund<sup>1</sup>

<sup>1</sup> Halliburton Landmark

### Summary

---

Interpreting seismic data enhances understanding of subsurface geological features, particularly for assisted fault interpretation. The results of assisted fault interpretation workflows can provide valuable information to optimize hydrocarbon production during drilling and stimulation treatments. However, given the complexity of seismic data such workflows can generate incorrect or misleading interpretations, such as discontinuous fault segments and mispositioned fault planes, particularly when deep-learning convolutional neural networks are used. Fault extraction results often face difficulties locating the fault plane where low reflectivity or signal-to-noise ratio exists. In this abstract, a novel approach is introduced that implements a super-resolution generative adversarial network to help improve the resolution of fault prediction results. Synthetic fault data were generated to train an adversarial model, which was then applied to different field data sets. This approach could serve as a standard post-processing workflow to decrease the uncertainty as part of an assisted fault interpretation approach and provides an efficient method of helping improve the fidelity of fault prediction results.

## Introduction

Deep learning-based approaches to automatic fault detection have grown more popular during the previous few years, demonstrating the potential to save significant interpretation time for geoscientists. However, fault prediction results from deep learning are often characterized by low resolution fault probability volumes that can extend a fault plane image out of its true range. Additionally, the low resolution of these fault prediction results smears the area where to locate the true fault. Clarifying these data using a traditional amplitude threshold scheme (Ferguson et al., 2010) could reject useful fault information, resulting in an incomplete fault segment. In this abstract, a weighted generative adversarial network (GAN) is implemented to help improve the fidelity of fault prediction results.

GANs (Goodfellow et al., 2014) are deep neural net architectures composed of two networks: the generator, which generates new data instances, and the discriminator, which evaluates them for authenticity. This adversarial model can automatically discover and learn the patterns in input data and mimic data distribution. GANs have been implemented in exploration geophysics to help geoscientists better understand subsurface structures and provide useful information for seismic interpretation. Alwon (2018) demonstrated the applicability of GANs for seismic processing by performing applications such as noise attenuation and trace interpolation. Picetti et al. (2018) also demonstrated the application of GANs for seismic imaging by showing that they can help turn low-quality migrated images into high-quality images, as if the acquisition geometry were much denser than in the input. GANs can also help turn a migrated image into the perspective deconvolved reflectivity image. Lu et al. (2018) presented an application that used GANs to sharpen seismic images before a fault identification workflow by helping eliminate blurry clouds of low probability values. Ledig et al. (2016) introduced a super-resolution approach using a GAN to improve the resolution of photo images. During their training, a high resolution (HR) image is downsampled to a low resolution (LR) image. A GAN generator then upsamples the LR images to super-resolution images.

In this abstract, a super-resolution GAN system is trained with synthetic fault labels. The trained GAN is applied to a field data set to clarify the fault probability map and help improve fault prediction accuracy. An image histogram equalization matrix is added to scale up the weak amplitude of the local patterns. The scaled GAN is able to enhance the weak features whilst keeping the strong features in an adversarial model. This approach can be implemented as a post-processing workflow to help eliminate the cloudy effects where low probability exists and help improve the resolution and clarify the fault probability map. This GAN model was applied to different field data sets, improving the resolution of their fault probability maps.

## Method

The workflow used is designed in two steps. The first step involves model training, which uses synthetic fault plane data, or HR images (HRI), with the exact fault position known to train the adversarial model. The generator takes downsampled synthetic fault planes, or LR images (LRI), as input and generates new fault planes, or super-resolution images (SRI), that are then fed into the discriminator alongside HRI. The discriminator attempts to authenticate a group of SRIs compared to a group of HRIs (Figure 1). Both networks attempt to optimize a different and opposing objective function as a minimax game, or zero-sum noncooperative game. At the end, when the discriminator and generator reach a Nash equilibrium (Nash, 1950), the discriminator is unable to distinguish SRI from HRI, and the adversarial model is successfully trained and saved for further processing.

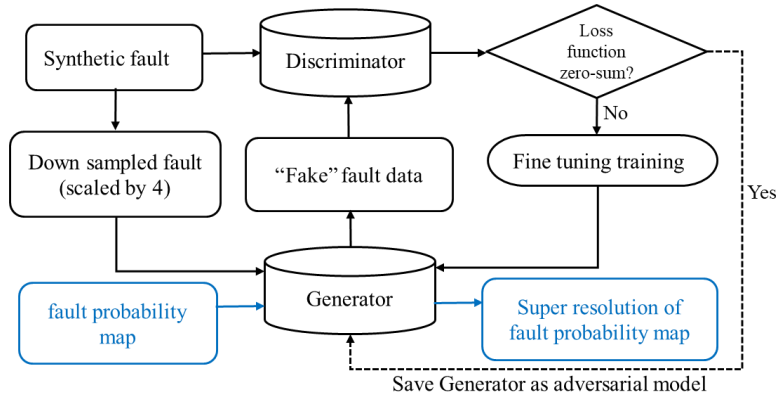


**Figure 1** Flowchart of super-resolution GAN to distinguish fault planes. Blue diagram shows the second step to helping predict the super-resolution fault probability map.

The difficulty in training a GAN is attributed to the loss function of the GAN architecture. The GAN can train two networks—the generator and discriminator—simultaneously. The discriminator model is updated as a normal deep-learning neural network; however, the generator uses the discriminator as the loss function, which is implicit and learned during the training process. During training, the generator loss is the sum of content loss and pixel-to-pixel mean loss using the mean square error (MSE) between the HRI and SRI. The perceptual loss function, which is vital for the performance of the generator network, is designed as

$$Loss^{SRI} = loss_{MSE}^{SRI} + \alpha * loss_{Adversarial}^{SRI}$$

where  $\alpha$  is a weighting factor. Here:

$$loss_{MSE}^{SRI} = \frac{1}{r^2 * w * h} \sum_{x=1}^{rw} \sum_{y=1}^{rh} (fault_{x,y}^{HRI} - fault_{x,y}^{SRI})^2$$

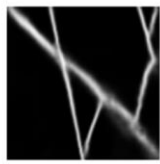





$$loss_{Adversarial}^{SRI} = \sum_{n=1}^N -\log(P(fault^{SRI}))$$

where  $loss_{MSE}^{SRI}$  represents pixel-wise MSE loss function,  $w$  and  $h$  represent filter width and height,  $r$  is the downsampled factor, which is 4 in these tests,  $loss_{Adversarial}^{SRI}$  represents the adversarial loss component, which helps the GAN favor solutions that reside on the manifold of natural images (Ledig et al., 2016), and  $P(fault^{SRI})$  is the probability the reconstructed fault plane is the same as the original fault planes, or HRI.

The second step involves prediction where fault prediction data are applied as input for the adversarial generator model, which generates super-resolution fault data and enhances the probability map where low probability exists. The trained adversarial model can be applied to other survey areas without retraining. Therefore, this GAN architecture could serve as a standard workflow to decrease the uncertainty as part of an automatic fault interpretation approach and provides an efficient method of helping improve the fidelity of fault prediction results.

## Examples

A synthetic data generator was implemented to generate synthetic fault planes to be used as training data to feed into the GAN model. During training, original fault data are imported to the discriminator while the degraded version of synthetic fault data are considered “fake fault data” and imported to the generator. When the discriminator is not able to distinguish fault data generated from the generator from the original fault map, the generator is saved as the final model. Next, that model is applied to a fault-probability volume generated using a convolutional neural network (CNN) method to produce the final refined fault map. Figure 2 shows a synthetic example where this GAN approach helps successfully improve the image resolution and better identifies thin fault segments.

Input	Output	Ground Truth
		
		

**Figure 2** Implementation of a GAN for synthetic fault planes. Left: predicted fault planes from CNN; a fuzzy or cloudy effect can clearly be observed, which represents low probability of predicted fault planes. Middle: result of predicted fault planes after being processed by the GAN. Right: original true fault plane used as training data.

The trained GAN model was further tested on a data set from offshore Australia (Indian 3D 2000 MSS). First, a deep-learning CNN was implemented to help predict 3D fault planes in this faulted area. The predicted 3D fault plane volume is then split into multiple small cubes ( $128 \times 128 \times 128$ ) and used as input data to feed into the GAN model. Figure 3 shows a comparison of the fault prediction results before GAN and after GAN along an inline direction. It was observed that fault planes reconstructed by the super-resolution GAN produce much thinner and clearer segments. The fuzzy and cloudy effects are removed from the original prediction result, providing a clearer fault probability map.

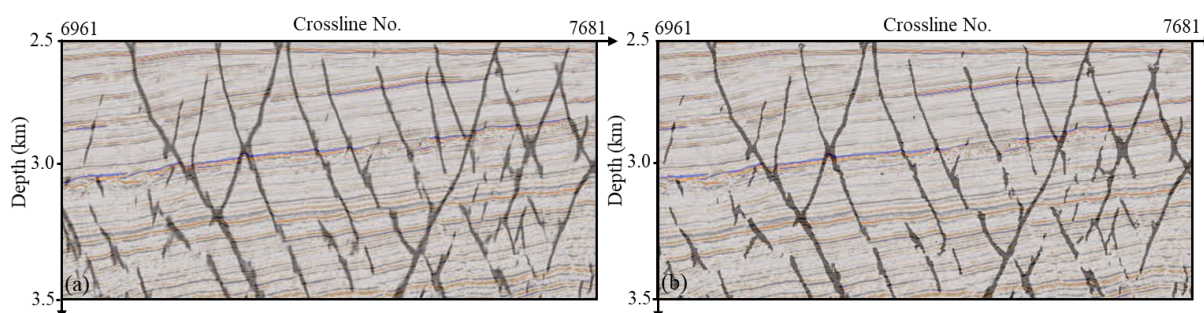


**Figure 3** Comparison of (a) predicted fault planes by CNN and (b) super resolution of fault planes processed by GAN. The GAN successfully removes fuzzy and cloudy effects without loss of accuracy.

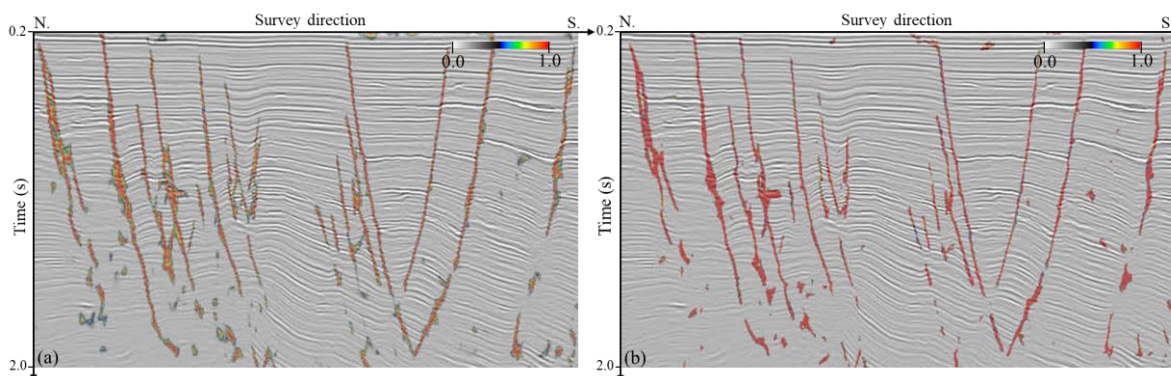


**Figure 4** Comparison of fault probability maps; (a) original map predicted using CNN; (b) map post-processed by the trained GAN model. The GAN effectively reconstructed and improved prediction results, enhancing fault probabilities where low probability existed in the original.

The trained GAN model can be applied to different survey areas to enhance the resolution of fault prediction results without retraining. Figure 4 shows another test example on the OPUNAKE3D data set from the Taranaiki basin offshore New Zealand. The trained GAN model was again directly applied to fault prediction results generated using a deep-learning method. Figure 4(a) shows original prediction results from the deep-learning neural network. The fault probability map ranges from 0.4 to 1.0 with variable rainbow color, which represents the unmodified data-driven estimate of confidence in the fault interpretation process. Figure 4(b) shows a fault probability map post-processed by the trained GAN model. The fault probability map is reconstructed, and noticeably enhanced, by the GAN model, with improved probability scores closer to 1, which brings advantage to analyze fault orientation and build fault discretization model. Notice that this GAN model only enhances fault probabilities where low values already exist; it does not generate new (false) fault segments. This new approach results in more detailed structural delineation, which, in turn, can increase the likelihood of technical and economic success with regard to discovering hydrocarbon accumulations.

## Conclusions

In this abstract, a post-processing workflow by training a GAN system to enhance the resolution of fault probability maps is introduced. Synthetic fault data were used as training data to train a modified GAN system, and then the trained GAN model was applied to two different field data sets. The results indicate that the GAN is capable of reconstructing the prediction map and enhancing and clarifying data where low probability exists, it also shows the potential benefits to generate thinned fault likelihood over other post-processing method, such as amplitude threshold method. This adversarial model could be applied to many other areas of seismic data processing and interpretation, such as domain transfer, reconstruction of missing traces, anomaly detection, etc.

## Acknowledgements

The authors thank the Australian Government and New Zealand Petroleum and Minerals for providing the seismic data used in this research.

## References

- Alwon, S. [2018] Generative adversarial networks in seismic data processing, SEG Annual Meeting, Extended Abstracts, 1991–1995.
- Ferguson, C., Avu, A., Schofield, N. and Paton, G., [2010] Seismic analysis workflow for reservoir characterization in the vicinity of salt, *The First Break*, V28, 107-113.
- Goodfellow, I., Pouget-Abadie, J., Mirza, M., Xu, B., Warde-Farley, D., Ozair, S., Courville, A., and Bengio, Y. [2014] Generative adversarial networks, *Proceedings of the international conference on neural information processing systems (NIPS 2014)*, 2672–2680.
- Ledig, C., Theis, L., Huszar, F., Caballero, J., Cunningham, A., Acosta, A., Aitken, A., Tejani, A., Totz, J., Wang, Z., and Shi, W. [2016] Photo-realistic single image super-resolution using a generative adversarial network, arXiv:1609.04802.
- Lu, P., Morris, M., Brazell, S., Comiskey, C., and Xiao, Y, [2018] Using generative adversarial networks to improve deep-learning fault interpretation networks, *The Leading Edge*, V37, 562–632.
- Nash, J., [1950] Equilibrium points in n-person games, *Proceedings of the National Academy of Sciences*, V36, 48–49.
- Picetti, F., Lipari, V., Bestagini, P., Tubaro, S., and Milano, P., [2018] A generative adversarial network for seismic imaging applications, SEG Annual Meeting, Extended Abstracts, 2231–2235.